Persistent acceleration of positrons in a nonstationary shock wave

メタデータ	言語: English 出版者: 公開日: 2012-11-29 キーワード (Ja): キーワード (En): 作成者: Hasegawa, Hiroki, Kato, Ken, Ohsawa, Yukiharu メールアドレス: 所属:
URL	http://hdl.handle.net/10655/8963

This work is licensed under a Creative Commons Attribution-NonCommercial-ShareAlike 3.0 International License.

AIP Physics of Plasmas

Persistent acceleration of positrons in a nonstationary shock wave

Hiroki Hasegawa, Ken Kato, and Yukiharu Ohsawa

Citation: Phys. Plasmas **12**, 082306 (2005); doi: 10.1063/1.2009507
View online: http://dx.doi.org/10.1063/1.2009507
View Table of Contents: http://pop.aip.org/resource/1/PHPAEN/v12/i8
Published by the American Institute of Physics.

Related Articles

Kr II laser-induced fluorescence for measuring plasma acceleration
Rev. Sci. Instrum. 83, 103111 (2012)

Computational fluid dynamics and frequency-dependent finite-difference time-domain method coupling for the interaction between microwaves and plasma in rocket plumes
Phys. Plasmas 19, 102112 (2012)

Interaction features of different propellants under plasma impingement
J. Appl. Phys. 112, 063303 (2012)

Ion velocity and plasma potential measurements of a cylindrical cusped field thruster
J. Appl. Phys. 111, 093303 (2012)

Three-dimensional particle-in-cell simulation of discharge characteristics in cylindrical anode layer hall plasma accelerator
Phys. Plasmas 19, 043507 (2012)

Additional information on Phys. Plasmas

Journal Homepage: http://pop.aip.org/
Journal Information: http://pop.aip.org/about/about_the_journal
Top downloads: http://pop.aip.org/features/most_downloaded
Information for Authors: http://pop.aip.org/authors

ADVERTISEMENT

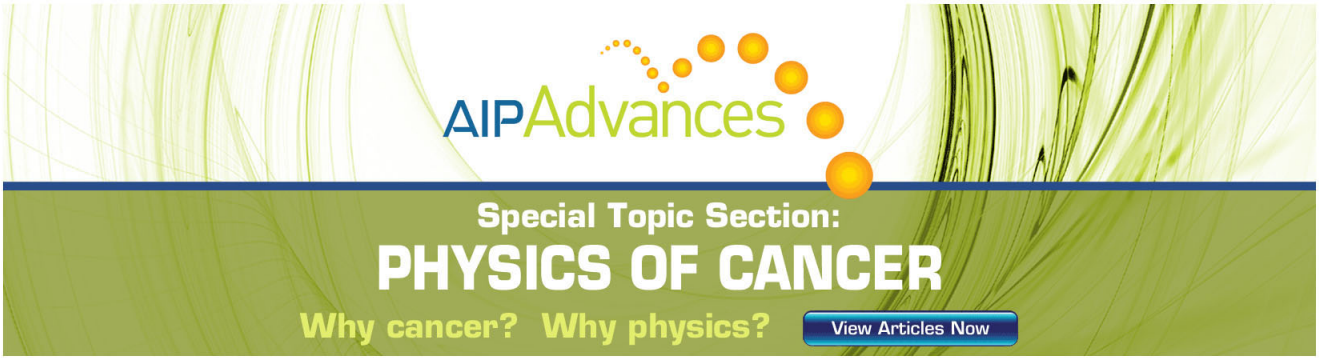

Downloaded 29 Nov 2012 to 133.75.110.124. Redistribution subject to AIP license or copyright; see http://pop.aip.org/about/rights_and_permissions

Persistent acceleration of positrons in a nonstationary shock wave

Hiroki Hasegawa[a)]
National Institute for Fusion Science, Toki 509-5292, Japan

Ken Kato and Yukiharu Ohsawa[b)]
Department of Physics, Nagoya University, Nagoya 464-8602, Japan

(Received 18 April 2005; accepted 8 July 2005; published online 12 August 2005)

Long-time evolution of positrons accelerated in an oblique shock wave in an electron-positron-ion plasma is studied with relativistic, electromagnetic, particle simulations. In the early stage, some positrons move nearly parallel to the external magnetic field in the shock transition region and gain energy from the parallel electric field. The acceleration can become stagnant owing to the deformation of the wave profile. After the recovery of the shock profile, however, the acceleration can start again. By the end of simulation runs, $\omega_{pe}t=5000$, positron Lorentz factors reached values ~ 2000. In this second stage, three different types of acceleration are found. In the first type, the acceleration process is the same as that in the early stage. In the second type, positrons make gyromotions in the wave frame and gain energy mainly from the perpendicular electric field. In the third type, particle orbits are similar to curtate cycloids. Theoretical estimate for this energy increase is given. © *2005 American Institute of Physics*. [DOI: 10.1063/1.2009507]

I. INTRODUCTION

Particle simulations show that a magnetosonic shock wave propagating obliquely to an external magnetic field in an electron-positron-ion (epi) plasma can accelerate some positrons[1,2] as well as electrons[3,4] and ions.[5–15] Because the positron mass is small, a shock wave in an epi plasma can easily reflect thermal positrons along the magnetic field with its electric field. When the shock propagation speed v_{sh} is close to $c\cos\theta$, where c is the speed of light and θ is the angle between the external magnetic field $\boldsymbol{B}_0$ and the wave normal, these positrons can become ultrarelativistic, staying in the shock transition region.

This mechanism could be important, for instance, around pulsars,[16,17] where positrons are expected to exist and the magnetic fields are strong. Since the magnetic fields and plasma density vary with the distance from a pulsar, and since shock waves can propagate with various angles θ, there would be regions where the condition $v_{sh}\sim c\cos\theta$ is satisfied.

A theory giving the zeroth- and first-order velocities of particles accelerated with this mechanism has been developed.[1,18] The zeroth-order velocity $\mathbf{v}_0$ is nearly parallel to $\boldsymbol{B}_0$, which is consistent with the simulation result. The time rate of change of the Lorentz factor γ of an accelerated positron is proportional to $(\boldsymbol{E}\cdot\boldsymbol{B}_0)$, where $\boldsymbol{E}$ is the wave electric field at particle positions. The first-order velocity $\mathbf{v}_1$, which is a small perturbation to $\mathbf{v}_0$, makes elliptic motions with frequencies $\omega\simeq(\boldsymbol{B}/B_0\cdot\mathbf{v}_0/c)(\Omega_p/\gamma_0)$, where $\boldsymbol{B}$ is the total magnetic field, Ω_p is the nonrelativistic gyrofrequency of positrons in the external magnetic field $\boldsymbol{B}_0$, and γ_0 is the zeroth-order Lorentz factor. This first-order theory accounted for the perturbation motions and frequencies observed in the simulations.

In the simulations in a Letter paper,[1] positron Lorentz factors reached values $\gamma\sim 600$, with runs up to $\omega_{pe}t\sim 2000$, where ω_{pe} is the electron plasma frequency. In Ref. 2, then, the parameter dependence of this acceleration was studied in detail with simulations. For a fixed propagation angle $\theta=42°$, high-energy positrons with $\gamma\gtrsim 200$ were observed in the shock speed range of $0.9\lesssim v_{sh}/(c\cos\theta)\lesssim 1.1$. Also, for a fixed propagation speed $v_{sh}/c=0.73$, positrons with $\gamma\gtrsim 200$ were observed in the angle range of $36<\theta<47$. The maximum energy increases with increasing ion-to-electron mass ratio; the above results were obtained with simulations with $m_i/m_e=100$. The acceleration is effective when the positron-to-electron density ratio is rather low, $n_{p0}/n_{e0}\lesssim 0.1$.

In these studies,[1,2] the energy rise seemed to have almost stopped near the end of the simulation runs. In the present paper, we study the evolution of shock waves and particle motions for a much longer time. It is then found that, after the plateau in the energy increase, the positron acceleration recovers. The energization processes are much more persistent than was expected in Refs. 1,2. We report the simulation results of these long acceleration processes.

In Sec. II, by using a one-dimensional (one space coordinate and three velocity components), relativistic, electromagnetic particle simulation code, we investigate particle motions in an oblique shock wave in an epi plasma. We make the system length twice as long as the previous one[1] and follow the shock wave up to $\omega_{pe}t=5000$. In the early phase of the simulation, positrons reflected by the shock wave are accelerated along the magnetic field. Then, the acceleration becomes stagnant; $d\gamma/dt$ is greatly reduced. This arises from the deformation of the wave profile due to the nonstationarity of the shock wave. After the recovery of the wave form, the acceleration begins again. (Stationary finite-amplitude waves are known.[19–23] Generally, however, large-amplitude waves are nonstationary.) In this second stage of the rise in γ, we find three different types of motions in

[a)]Electronic mail: hasegawa@tcsc.nifs.ac.jp
[b)]Electronic mail: ohsawa@nagoya-u.jp

 © 2005 American Institute of Physics

Downloaded 29 Nov 2012 to 133.75.110.124. Redistribution subject to AIP license or copyright; see http://pop.aip.org/about/rights_and_permissions

positrons suffering acceleration. In the first type, particles move nearly parallel to $\boldsymbol{B}_0$ as in the early phase; its mechanism is thus the same as that discussed in Ref. 1. In the second type, particles make gyromotions in the wave frame with gyroradii greater than the shock transition region, absorbing energy from the transverse electric field. We can account for the energization of the second type by applying the theory for the incessant acceleration of relativistic particles, which was originally developed for energetic ions.[24] In the third type, particle orbits are similar to curtate cycloids in the wave frame. In each type, Lorentz factors reach values $\gamma \sim 2000$ by the end of the run.

The energy increase in the third type, which is newly found in the present paper, is analytically discussed in Sec. III. A summary of our work is given in Sec. IV.

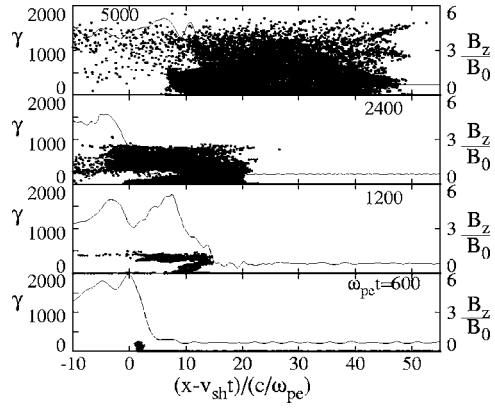

FIG. 1. Positron phase-space plots $(x-v_{sh}t, \gamma)$ and profiles of B_z at various times.

II. SIMULATION RESULTS

We investigate long-time behavior of positrons accelerated by an oblique shock wave in an epi plasma, by using a one-dimensional (one space coordinate and three velocities), relativistic, electromagnetic particle code with full particle dynamics. Shock waves propagate in the positive x direction in an external magnetic field $\boldsymbol{B}_0 = B_0(\cos\theta, 0, \sin\theta)$. For the method of particle simulations of shock waves, see Refs. 3, 7, and 25.

The simulation parameters are as follows. The total system length is $L = 16\,384\Delta_g$, where Δ_g is the grid spacing; this system length is twice as long as that in the previous simulations of the positron acceleration.[1] The number of simulation electrons is $N_e \simeq 1.23 \times 10^6$; the ion-to-electron mass ratio is $m_i/m_e = 100$ with $m_p = m_e$; the propagation angle is $\theta = 42^\circ$; and the ratio of gyro and plasma frequencies of electrons is $|\Omega_e|/\omega_{pe} = 3.0$, where $\Omega_e = -eB_0/(m_e c)$ and $\omega_{pe}^2 = 4\pi n_{e0} e^2/m_e$ with n_{e0} as the electron density averaged over the entire plasma region. The light speed is $c/(\omega_{pe}\Delta_g) = 4.0$. The thermal velocities in the upstream region are $v_{T_e}/(\omega_{pe}\Delta_g) = v_{T_p}/(\omega_{pe}\Delta_g) = 0.33$ and $v_{T_i}/(\omega_{pe}\Delta_g) = 0.033$, respectively. The positron-to-electron density ratio is taken to be $n_p/n_e = 0.02$. The Alfvén speed is then $v_A/(\omega_{pe}\Delta_g) = 1.2$. The time step is $\omega_{pe}\Delta t = 0.01$. (Here, the thermal speeds are defined by $\sqrt{T/m}$. In Ref. 1, however, the thermal speeds defined by $\sqrt{2T/m}$ and normalized to c were mentioned. The thermal speeds in the present simulation are the same as those in Ref. 1 if we use the same definition and normalization.)

A. Overview of positron acceleration

Figure 1 displays positron phase-space plots $(x-v_{sh}t, \gamma)$ and profiles of B_z at various times of a shock wave with a propagation speed $v_{sh} = 2.43 v_A$. In the early stage, some positrons are being accelerated in the shock transition region; at $\omega_{pe}t = 600$, the maximum γ is ~ 250. Around $\omega_{pe}t = 1200$, the spatial distribution of accelerated positrons is quickly spreading. In contrast, the increase in the particle energy is slow around this time; later, this will be shown more clearly. After the plateau, the maximum energy begins to steadily grow again, reaching the value $\gamma \sim 2000$ by $\omega_{pe}t = 5000$. We show in Fig. 2 the energy distribution functions of positrons. The maximum energy and the number of high-energy particles both go up with time. Here, the black bars indicate the particles that have been accelerated to energies $\gamma > 200$ by $\omega_{pe}t = 800$; i.e., by the time of the plateau of energy increase. We find both white and black bars in the high-energy region after the stagnation, $\omega_{pe}t \gtrsim 2400$. That is, either the positrons with $\gamma > 200$ at $\omega_{pe}t = 800$ or the ones with $\gamma < 200$ at that time can be accelerated later.

The spreading of the x positions around $\omega_{pe}t = 1200$ is due to the deformation of the field profiles; large-amplitude shock waves are not stationary. We show in Fig. 3 the profiles of B_z and E_x, the longitudinal electric field. At $\omega_{pe}t = 1200$ and $\omega_{pe}t = 1600$, the fields in the main pulse region are weak and diffusive compared with those at the other times.

Next, we study individual particle motions. We find three different types of acceleration motions.

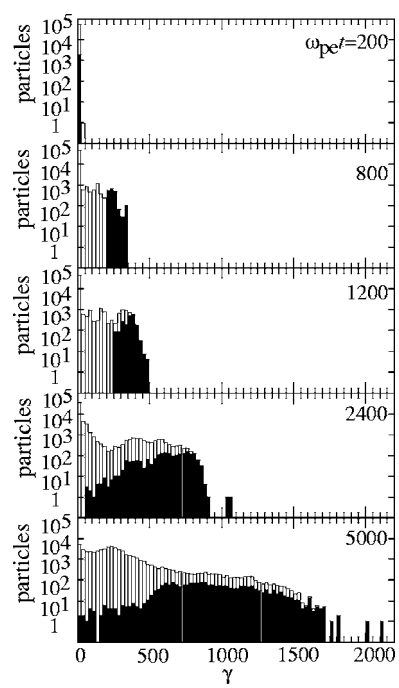

FIG. 2. Evolution of positron energy distribution. The black bars indicate the particles that have energies $\gamma > 200$ at $\omega_{pe}t = 800$.

Downloaded 29 Nov 2012 to 133.75.110.124. Redistribution subject to AIP license or copyright; see http://pop.aip.org/about/rights_and_permissions

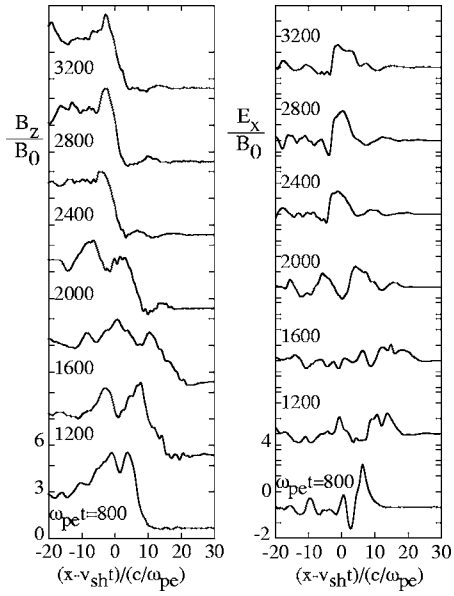

FIG. 3. Profiles of B_z and E_x at various times. The fields are weak and diffusive in the main pulse region at $\omega_{pe}t=1200$ and $\omega_{pe}t=1600$.

B. Type 1: Nearly parallel acceleration

Figure 4 displays time variations of γ and $\mathbf{v}$ of an accelerated positron. After the encounter with the shock wave, γ continues to grow until $\omega_{pe}t \simeq 1000$. The acceleration mechanism for this early phase was discussed in detail in the previous paper;[1] positrons move nearly parallel to the external magnetic field and gain energy with the increase rate,

$$\frac{d\gamma}{dt} = \Omega_p \frac{c\cos\theta}{v_{sh}} \frac{(\boldsymbol{E}\cdot\boldsymbol{B})}{(\boldsymbol{B}\cdot\boldsymbol{B}_0)}. \tag{1}$$

(For a stationary one-dimensional wave, we have $\boldsymbol{E}\cdot\boldsymbol{B} = \boldsymbol{E}\cdot\boldsymbol{B}_0$.) From $\omega_{pe}t \simeq 1000$ to $\omega_{pe}t \simeq 2000$, γ does not increase much. In Ref. 1, the simulations were performed until $\omega_{pe}t \simeq 2000$. Hence, it was thought that the acceleration processes were almost finished. The present long-time simulation indicates, however, that after the plateau, the energy

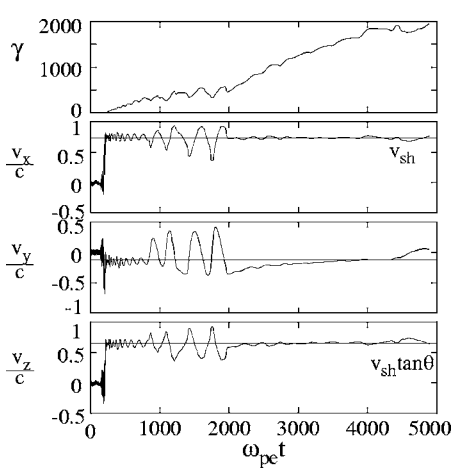

FIG. 4. Time variations of γ and $\mathbf{v}$ of a positron. This particle is accelerated nearly parallel to $\boldsymbol{B}_0$ for $\omega_{pe}t > 2000$ as well as in the early phase.

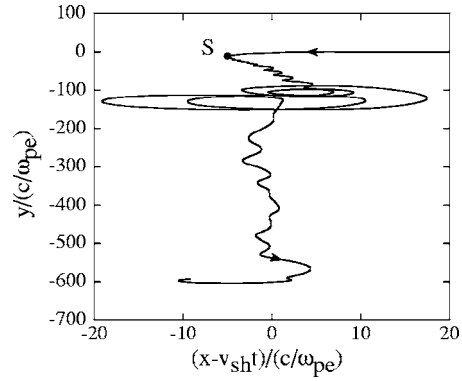

FIG. 5. Particle trajectory in the $(x-v_{sh}t, y)$ plane. The particle encounters the shock wave at point S.

starts to rise again at $\omega_{pe}t \sim 2000$. By the end of the simulation run, γ reaches the value of 2000.

The horizontal lines in the second to fourth panels show the velocities expected from the zeroth-order theory for the nearly parallel acceleration;[1,18] that is,

$$v_{x0} = v_{sh}, \tag{2}$$

$$\frac{v_{y0}}{c} = \frac{B_{x0}B_y\gamma_{sh}^{-2} - E_xB_{z0}(v_{sh}/c)}{B_{z0}B_z(v_{sh}/c) + B_{z0}^2\gamma_{sh}^2(v_{sh}/c)^3}, \tag{3}$$

$$\frac{v_{z0}}{c} = \frac{B_{x0}}{B_{z0}}\frac{c}{\gamma_{sh}^2 v_{sh}} \simeq \frac{v_{sh}}{c}\tan\theta, \tag{4}$$

where

$$\gamma_{sh} = (1 - v_{sh}^2/c^2)^{-1/2}. \tag{5}$$

We estimated $\mathbf{v}_0$ in Fig. 4 by using time-averaged field values at particle positions in the early phase $200 \leqslant \omega_{pe}t \leqslant 800$. Except for the period from $\omega_{pe}t \sim 1000$ to $\omega_{pe}t \sim 2000$, the values of v_x, v_y, and v_z are nearly constant and are close to the theoretically predicted ones (2)–(4). This suggests that the acceleration mechanism for $\omega_{pe}t \gtrsim 2000$ is the same as the one in the early phase.

Figure 5 shows the trajectory of this particle in the $(x - v_{sh}t, y)$ plane. Here, the point $x - v_{sh}t = 0$ corresponds to the position where B_z takes its maximum value on average. The width of the shock transition region is $\sim 7c/\omega_{pe}$ in this simulation (see Fig. 3). After the particle entered the shock wave (this moment is indicated by point S), its y position moved from $y/(c/\omega_{pe}) \simeq 0$ to $y/(c/\omega_{pe}) \simeq -100$. The particle then makes gyromotion a few times from $\omega_{pe}t \simeq 1000$ to $\omega_{pe}t \simeq 2000$. After the gyromotion, it begins to move in the negative y direction from $y/(c/\omega_{pe}) \simeq -200$ to $y/(c/\omega_{pe}) \simeq -600$, during which the particle suffers the acceleration nearly parallel to $\boldsymbol{B}_0$.

Figure 6 shows time variations of γ, γ_{HUO}, and $W_\perp$ of this particle. Here, γ_{HUO} is defined as

$$\gamma_{HUO} = \int \Omega_p \frac{c\cos\theta}{v_{sh}} \frac{(\boldsymbol{E}\cdot\boldsymbol{B})}{(\boldsymbol{B}\cdot\boldsymbol{B}_0)} dt, \tag{6}$$

where the integration is carried out along the particle trajectory. It represents the increase in γ in the case where the

Downloaded 29 Nov 2012 to 133.75.110.124. Redistribution subject to AIP license or copyright; see http://pop.aip.org/about/rights_and_permissions

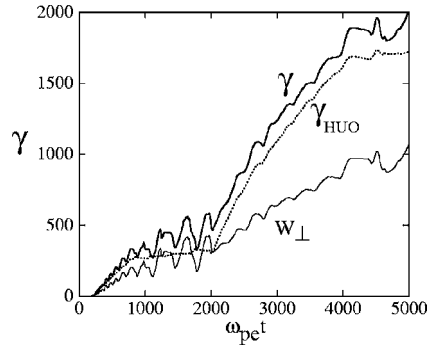

FIG. 6. Time variations of γ, γ_{HUO}, and $W_{\perp}$. The line of γ_{HUO} closely resembles that of γ.

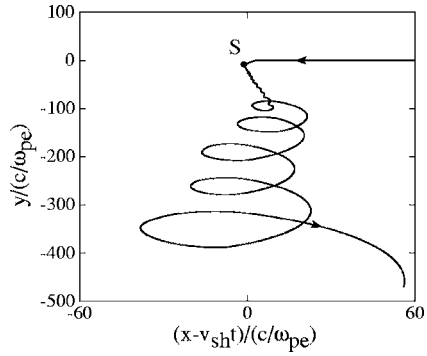

FIG. 8. Particle trajectory in the $(x-v_{\mathrm{sh}}t,y)$ plane. For $y/(c/\omega_{\mathrm{pe}})<-100$, the particle makes a prolate-cycloid-like motion.

acceleration is performed by the mechanism discussed by Hasegawa *et al.*[1] and Usami and Ohsawa.[1,18] The quantity $W_{\perp}$ is the work done by the electric field perpendicular to the magnetic field,

$$W_{\perp}=\frac{e}{m_e c^2}\int \boldsymbol{E}_{\perp}\cdot\boldsymbol{v}dt. \tag{7}$$

The shapes of γ and γ_{HUO} are quite similar; rise in the early phase, stagnation from $\omega_{\mathrm{pe}}t\simeq 1000$ to $\omega_{\mathrm{pe}}t\simeq 2000$, and the recovery of the rise after $\omega_{\mathrm{pe}}t\simeq 2000$. This acceleration is thus well accounted for by the theory presented in Refs. 1 and 18. On the other hand, $W_{\perp}$ is much smaller than the observed γ in this case, indicating that $\boldsymbol{E}_{\perp}$ does not play a major role in the acceleration.

C. Type 2: Perpendicular acceleration

Next, we show acceleration in association with gyromotions of energetic particles. Figure 7 displays time variations of γ and $\mathbf{v}$ of a positron suffering this type of energy multiplication. After the increase in the early phase, γ rises stepwise. For $\omega_{\mathrm{pe}}t\gtrsim 1000$, the three velocities oscillate with much larger amplitudes and much longer periods than those in the early phase. The energy jump occurs when v_y is positive, suggesting that the particle gains energy mainly from the transverse electric field E_y.[24] In the present example, we do not find a clear plateau period; after the acceleration nearly parallel to $\boldsymbol{B}_0$, the next energization processes quickly start.

Figure 8 shows that in the $(x-v_{\mathrm{sh}}t,y)$ plane, the particle makes a gyromotion for $y/(c/\omega_{\mathrm{pe}})\lesssim -100$, which corresponds to the time $\omega_{\mathrm{pe}}t\gtrsim 1000$. Figure 9 shows time variations of γ, γ_{HUO}, and $W_{\perp}$. The γ_{HUO} in this type significantly grows only in the early phase, while the shape of $W_{\perp}$ is quite similar to that of γ for $\omega_{\mathrm{pe}}t\gtrsim 1000$. The energy increase results from the gyromotion with large gyroradius, as in the incessant acceleration of fast ions.[24]

D. Type 3: Acceleration in curtate-cycloid-like orbit

In the third type (see Fig. 10), γ increases stepwise for $\omega_{\mathrm{pe}}t\gtrsim 2000$ as in type 2, while the amplitudes of the velocity oscillations for $\omega_{\mathrm{pe}}t\gtrsim 2000$ are much smaller than those in type 2. The energy goes up when v_x changes from the minima to maxima. As shown in Fig. 11, the particle trajectory resembles a curtate cycloid in the $(x-v_{\mathrm{sh}}t,y)$ plane for $y/(c/\omega_{\mathrm{pe}})\lesssim -200$. Figure 12 shows that γ, γ_{HUO}, and $W_{\perp}$ all show stepwise increase for $\omega_{\mathrm{pe}}t\gtrsim 2000$. Both γ_{HUO} and $W_{\perp}$ are considerably smaller than γ.

We will discuss the energy increase in type 3 in Sec. III.

III. ENERGY GAIN OF PARTICLES WITH CURTATE-CYCLOID-LIKE ORBIT

We estimate the energy jump of particles with orbits similar to a curtate cycloid. Simulations show that these par-

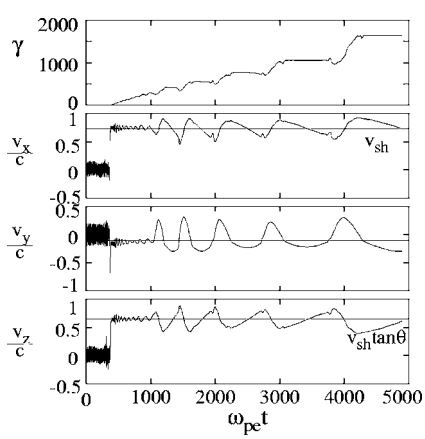

FIG. 7. Time variations of γ and $\mathbf{v}$ of a positron. For $\omega_{\mathrm{pe}}t>1000$, γ increases stepwise, and the velocities oscillate with large amplitudes. The jumps of γ occur when $v_y>0$.

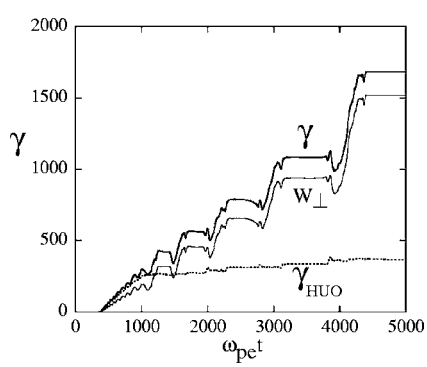

FIG. 9. Time variations of γ, γ_{HUO}, and $W_{\perp}$. Here, γ and $W_{\perp}$ have quite similar profiles for $\omega_{\mathrm{pe}}t>1000$.

Downloaded 29 Nov 2012 to 133.75.110.124. Redistribution subject to AIP license or copyright; see http://pop.aip.org/about/rights_and_permissions

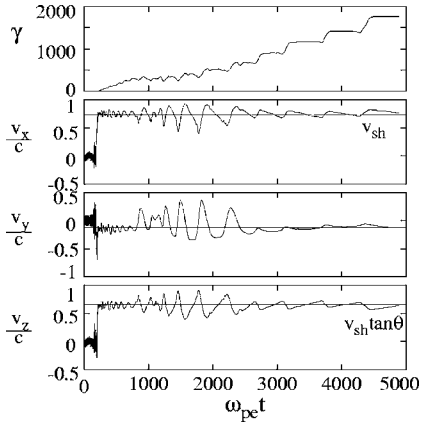

FIG. 10. Time variations of γ and $\mathbf{v}$ of a positron. The energy rises stepwise for $\omega_{pe}t>2000$, while the amplitudes of the velocity oscillations are small for $\omega_{pe}t>2500$.

ticles undergo energy jumps when v_x rises from its minima to maxima. They are impulsively pushed by strong longitudinal electric field E_x from time $t_{\min}$ to $t_{\max}$, where $t_{\min}$ and $t_{\max}$ denote the times of the minima and maxima of v_x, respectively. The energy jump in the laboratory frame is related to the energy and momentum in the wave frame through the Lorentz transformation,

$$m_pc^2[\gamma(t_{\max})-\gamma(t_{\min})]=\gamma_{\rm sh}m_pc^2[\gamma_w(t_{w\,\max})-\gamma_w(t_{w\,\min})]+\gamma_{\rm sh}v_{\rm sh}[p_{wx}(t_{w\,\max})-p_{wx}(t_{w\,\min})], \tag{8}$$

where the subscript w refers to the quantities in the wave frame (shock normal incident frame). With the aid of Eq. (5) and the relation

$$p_{wx}(t_{w\,\max})-p_{wx}(t_{w\,\min})=\gamma_{\rm sh}[p_x(t_{\max})-p_x(t_{\min})]-m_p\gamma_{\rm sh}v_{\rm sh}[\gamma(t_{\max})-\gamma(t_{\min})], \tag{9}$$

Eq. (8) becomes

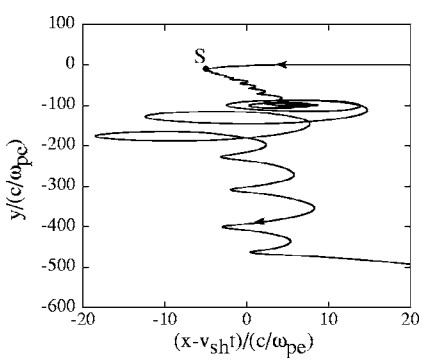

FIG. 11. Particle trajectory in the $(x-v_{\rm sh}t,y)$ plane. For $y/(c/\omega_{pe})<-200$, the particle makes curtate-cycloid-like motion.

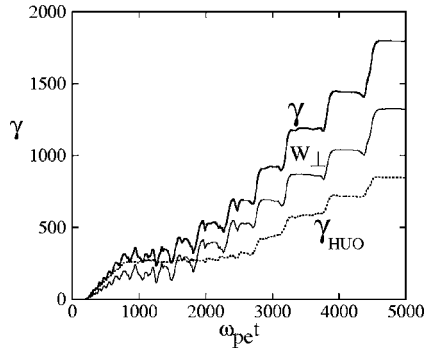

FIG. 12. Time variations of γ, $\gamma_{\rm HUO}$, and $W_\perp$. Here, both $W_\perp$ and $\gamma_{\rm HUO}$ are considerably smaller than γ.

$$m_pc^2\gamma_{\rm sh}^2[\gamma(t_{\max})-\gamma(t_{\min})]=\gamma_{\rm sh}m_pc^2[\gamma_w(t_{w\,\max})-\gamma_w(t_{w\,\min})]+\gamma_{\rm sh}^2v_{\rm sh}[p_x(t_{\max})-p_x(t_{\min})]. \tag{10}$$

In the wave frame, it holds that $E_{wz}=0$. In addition, the x position averaged over each period of the curtate-cycloid-like motion is nearly constant; we thus assume that $x_w(t_{w\,\min})\simeq x_w(t_{w\,\max})$. Then, since the electric field in the y direction is constant,

$$E_{wy0}=-(v_{\rm sh}/c)B_{wz0}, \tag{11}$$

the energy change in the wave frame is given as

$$m_pc^2[\gamma_w(t_{w\,\max})-\gamma_w(t_{w\,\min})]=e\int_{t_{w\,\min}}^{t_{w\,\max}}E_{wy0}v_{wy}dt_w=eE_{wy0}\delta y_w, \tag{12}$$

where δy_w is the change in y_w from $t_w=t_{w\,\min}$ to $t_w=t_{w\,\max}$. Because $y=y_w$ in the present circumstances, we can estimate the change in y as $\delta y_w=\delta y=v_{y0}(t_{\max}-t_{\min})$. By the use of the relations (11) and $B_{wz0}=\gamma_{\rm sh}B_{z0}$, Eq. (12) can be written as

$$m_pc^2[\gamma_w(t_{w\,\max})-\gamma_w(t_{w\,\min})]=-e\gamma_{\rm sh}v_{\rm sh}B_{z0}\delta y/c. \tag{13}$$

We thus find the jump in the Lorentz factor as

$$\gamma(t_{\max})-\gamma(t_{\min})=-\frac{v_{\rm sh}}{c^2}\frac{B_{z0}}{B_0}\Omega_pv_{y0}(t_{\max}-t_{\min})+\frac{v_{\rm sh}[p_x(t_{\max})-p_x(t_{\min})]}{m_pc^2}. \tag{14}$$

Let us compare Eq. (14) with the simulation result. The energy jump during the period from $\omega_{pe}t_{\min}=2703$ to $\omega_{pe}t_{\max}=2802$ in Fig. 12 is $\delta\gamma=213$, while Eq. (14) gives $\delta\gamma=212$; we have obtained this theoretical value by substituting the observed value $[p_x(t_{\max})-p_x(t_{\min})]/(m_pc)=264$. For v_{y0}, we have used the value $v_{y0}/c=-0.128$, which we obtained from Eq. (3) by averaging the field values over time from $\omega_{pe}t=2802$ to $\omega_{pe}t=4544$. Similarly, for the energy jumps for the periods from $\omega_{pe}t_{\min}=3129$ to $\omega_{pe}t_{\max}=3248$, from 3764 to 3900, and from 4365 to 4544, $\delta\gamma$'s in the simulation are 251, 269, and 362, respectively, while Eq.

Downloaded 29 Nov 2012 to 133.75.110.124. Redistribution subject to AIP license or copyright; see http://pop.aip.org/about/rights_and_permissions

(14) gives, in the same order, 255, 274, and 366. The values given by Eq. (14) are consistent with the simulation result.

IV. SUMMARY

We have numerically studied the long-time evolution of positron acceleration in a shock wave in a magnetized epi plasma. In Ref. 1, it was reported that positrons can be accelerated nearly parallel to the external magnetic field when $v_{\rm sh} \sim c \cos\theta$; at the end of the simulation run, the energy rise seemed to be almost stopped with $\gamma \sim 600$. In this paper, we have doubled the system length, $L = 16\,384\Delta_g$, and have observed the evolution of a shock wave and particle motion for a time period twice as long as that in Ref. 1.

It has then been found that the plateau of the energy increase is due to the deformation of the field profiles of the shock wave. After the field profiles have recovered, three different types of positron acceleration appeared. By the end of the simulation, $\omega_{\rm pe} t = 5000$, γ reached values ~ 2000.

In the first type, after short-period turbulent trajectories, motions nearly parallel to $\boldsymbol{B}_0$ are restored. In the second type, positrons make gyromotion in the wave frame with gyroradii greater than the width of the shock transition region and gain energy from the perpendicular electric field. We can understand this mechanism by applying the theory of the incessant acceleration of relativistic ions[24] to ultrarelativistic positrons with large gyroradii. In the third type, positron orbits are similar to curtate cycloids along the shock front. Theoretical estimate for the energy increase has been given for the third type acceleration.

ACKNOWLEDGMENTS

This work was supported in part by the joint research program of the Solar-Terrestrial Environment Laboratory, Nagoya University, and by the collaboration program of the National Institute for Fusion Science.

[1] H. Hasegawa, S. Usami, and Y. Ohsawa, Phys. Plasmas **10**, 3455 (2003).
[2] H. Hasegawa and Y. Ohsawa, Phys. Plasmas **12**, 012312 (2005).
[3] N. Bessho and Y. Ohsawa, Phys. Plasmas **6**, 3076 (1999).
[4] N. Bessho and Y. Ohsawa, Phys. Plasmas **9**, 979 (2002).
[5] D. Biskamp and H. Welter, Nucl. Fusion **12**, 663 (1972).
[6] D. W. Forslund, K. B. Quest, J. U. Brackbill, and K. Lee, J. Geophys. Res., [Oceans] **89**, 2142 (1984).
[7] Y. Ohsawa, Phys. Fluids **28**, 2130 (1985).
[8] B. Lembege and J. M. Dawson, Phys. Fluids B **1**, 1001 (1989).
[9] R. L. Tokar, S. P. Gary, and K. B. Quest, Phys. Fluids **30**, 2569 (1987).
[10] R. Z. Sagdeev and V. D. Shapiro, Zh. Eksp. Teor. Fiz. Pis'ma Red. **17**, 387 (1973) [JETP Lett. **17**, 279 (1973)].
[11] Y. Ohsawa, J. Phys. Soc. Jpn. **59**, 2782 (1990).
[12] M. A. Lee, V. D. Shapiro, and R. Z. Sagdeev, J. Geophys. Res., [Oceans] **101**, 4777 (1996).
[13] T. P. Armstrong, G. Chen, E. T. Sarris, and S. M. Krimigis, in *Study of Traveling Interplanetary Phenomena*, edited by M. A. Shea and D. F. Smart (Reidel, Dordrecht, 1977), p. 367.
[14] R. B. Decker, Space Sci. Rev. **48**, 195 (1988).
[15] M. Toida and Y. Ohsawa, Sol. Phys. **171**, 161 (1997).
[16] P. A. Sturrock, Astrophys. J. **164**, 529 (1971).
[17] T. Tanimori, K. Sakurazawa, S. A. Dazeley *et al.*, Astrophys. J. Lett. **492**, L33 (1998).
[18] S. Usami and Y. Ohsawa, Phys. Plasmas **11**, 3203 (2004).
[19] J. H. Adlam and J. E. Allen, Philos. Mag., Suppl. **3**, 448 (1958).
[20] L. Davis, R. Lüst, and A. Schlüter, Z. Naturforsch. A **13**, 916 (1958).
[21] Y. Ohsawa, Phys. Fluids **29**, 2474 (1986).
[22] C. S. Gardner and G. K. Morikawa, Commun. Pure Appl. Math. **18**, 35 (1965).
[23] T. Kakutani, H. Ono, T. Taniuti, and C. C. Wei, J. Phys. Soc. Jpn. **24**, 1159 (1968).
[24] S. Usami and Y. Ohsawa, Phys. Plasmas **9**, 1069 (2002).
[25] P. C. Liewer, A. T. Lin, J. M. Dawson, and M. Z. Caponi, Phys. Fluids **24**, 1364 (1981).

Downloaded 29 Nov 2012 to 133.75.110.124. Redistribution subject to AIP license or copyright; see http://pop.aip.org/about/rights_and_permissions